www.nature.com/ismej

ISME

ARTICLE

Biophotoelectrochemical process co-driven by dead microalgae and live bacteria

Shanshan Chen[1], Jin Chen[2], Lanlan Zhang[1], Shaofu Huang[2], Xing Liu[2], Yuting Yang[1], Tiangang Luan[1], Shungui Zhou[2]✉, Kenneth H. Nealson[3] and Christopher Rensing[2]

Anaerobic reduction processes in natural waters can be promoted by dead microalgae that have been attributed to nutrient substances provided by the decomposition of dead microalgae for other microorganisms. However, previous reports have not considered that dead microalgae may also serve as photosensitizers to drive microbial reduction processes. Here we demonstrate a photoelectric synergistic linkage between dead microalgae and bacteria capable of extracellular electron transfer (EET). Illumination of dead *Raphidocelis subcapitata* resulted in two-fold increase in the rate of anaerobic bioreduction by pure *Geobacter sulfurreducens*, suggesting that photoelectrons generated from the illuminated dead microalgae were transferred to the EET-capable microorganisms. Similar phenomena were observed in NO_3^- reduction driven by irradiated dead *Chlorella vulgaris* and living *Shewanella oneidensis*, and Cr(VI) reduction driven by irradiated dead *Raphidocelis subcapitata* and living *Bacillus subtilis*. Enhancement of bioreduction was also seen when the killed microalgae were illuminated in mixed-culture lake water, suggesting that EET-capable bacteria were naturally present and this phenomenon is common in post-bloom systems. The intracellular ferredoxin-$NADP^+$-reductase is inactivated in the dead microalgae, allowing the production and extracellular transfer of photoelectrons. The use of mutant strains confirmed that the electron transport pathway requires multiheme cytochromes. Taken together, these results suggest a heretofore overlooked biophotoelectrochemical process jointly mediated by illumination of dead microalgae and live EET-capable bacteria in natural ecosystems, which may add an important component in the energetics of bioreduction phenomena particularly in microalgae-enriched environments.

The ISME Journal (2023) 17:712–719; https://doi.org/10.1038/s41396-023-01383-3

INTRODUCTION

Algal blooms occur as a result of nutrient input in oceanic upwelling areas around the world, and in lakes, as a result of eutrophication [1]. When these blooms crash, they leave behind huge numbers of dead microalgal cells that often lead to poor water quality and anoxic conditions [2–4] in which the dead microalgae promote denitrification, methane production, and release of heavy metals at the sediment/soil–water interface [5–7]. Previous studies have attributed the above effects to the decay of lysed microalgal cells providing abundant organic carbon, nitrogen and phosphorus that serve as nutrients for other microorganisms [3, 8].

When the incident light energy is greater than the band gap between the valence band and the conduction band of photosensitizers including metal oxides/sulfides, S^0, anthraquinone and dissolved organic matter, photoelectron-hole pairs can be generated and energy has been shown to be released to trigger redox reactions [9–12]. Some of these strongly reducing photoelectrons can be harvested by non-phototrophic microorganisms and drive microbial processes such as nitrate reduction, methane production and carbon/nitrogen fixation [13–17]. Moreover, the energy source generated by the light-excited photoelectrons could also be used by microorganisms to reconstruct their microbial communities to adapt to the environment, wherein the bacteria capable of extracellular electron transfer (EET) would become more abundant [9, 18, 19].

The illumination of dead microalgal cells has been shown to lead to the photocatalytic oxidation of organic pollutants, since they are able to generate reactive oxygen species including the hydroxyl radical, singlet oxygen, hydrogen peroxide and the superoxide radical [20, 21]. However, whether the dead microalgae might be able to provide reducing photoelectrons and whether the photoelectrons can be utilized by other microorganisms has not, to our knowledge, been reported. If so, it may be possible that photoelectrons produced by dead microalgal cells are able to drive some microbial anaerobic processes via a novel synergistic mechanism of dead algae with EET-capable bacteria that alters the energetics of such systems. To this end, the aim of this work was to test the hypothesis that anaerobic reductive processes can be driven by photoelectrons provided by illumination of dead microalgae and delivered to live EET-capable bacteria. A chlorophyte, *Raphidocelis subcapitata* was used as the microalga [20], while *Geobacter sulfurreducens* was taken as the bacterium since it is capable of absorbing photoelectrons [22, 23], and methyl orange (MO) reduction was chosen as the model anaerobic

[1]Guangdong Provincial Key Laboratory of Water Quality Improvement and Ecological Restoration for Watersheds, School of Ecology, Environment and Resources, Guangdong University of Technology, Guangzhou, China. [2]Fujian Provincial Key Laboratory of Soil Environmental Health and Regulation, College of Resources and Environment, Fujian Agriculture and Forestry University, Fuzhou, China. [3]Department of Earth Science, University of Southern California, Los Angeles, CA, USA. ✉email: sgzhou@fafu.edu.cn

Received: 7 August 2022 Revised: 8 February 2023 Accepted: 10 February 2023
Published online: 23 February 2023

reduction process [24]. In separate experiments, lake water was collected to demonstrate that the photoelectric mechanism of dead microalgae also works in a sunlit mixed-bacteria environment. Here, we report an overlooked synergistic linkage between dead algae and live bacteria in natural ecosystems, and use mutant and biophotoelectrochemical-cell experiments to further analyze the mechanism of these biophotoelectrochemical processes occurring between them.

MATERIALS AND METHODS

Microorganisms and cultivation conditions

R. subcapitata (152521, purchased from CAROLINA (https://www.carolina.com)) was incubated in a sterilized soil extract medium under aerobic condition at 22 °C, illuminated with cool white fluorescent tubes (light intensity = 2 mW/cm^2) with a light-dark duration of 16:8 h [20]. After 7 days of cultivation, microalgal cells were centrifuged at 9000 × *g* for 10 min at 4 °C, washed with sterile deionized water, and heated in a water bath at 65 °C for 30 min for the dead microalgae treatment. In order to make sure that all cells were inactivated, growth curves based on OD_{680} and dry biomass weight [25] were measured (Fig. S1), and cells were stained by SYTOX Green (Thermo Fisher) and observed by fluorescence microscopy (Axio Imager A2, ZEISS, Germany) [26] (Fig. S2). The stabilized growth curves and green fluorescence emitted by dead cells demonstrated that cells were inactivated after the 65 °C-water bath. The naturally dying microalgae were obtained by placing the microalgae in the dark for 21 days. Since 21 days was a long time and we needed plenty of dead microalgae cells, the 65 °C-inactivated method was chosen in order to quickly obtain dead microalgal cells within 30 min that possessed reductase activities and photocurrents similar to those of the naturally occurring dead microalgae (Figs. S3 and S4).

G. sulfurreducens PCA (51573, purchased from the ATCC (https://www.atcc.org)) and its gene-deletion mutants (*G. sulfurreducens* Δ*omcZ*, *G. sulfurreducens* Δ*omcS*, *G. sulfurreducens* Δ*omcB* and *G. sulfurreducens* Δ*pilA*) were constructed by Xing Liu [23, 27] were cultured in sterilized NBAF medium with 10 mM acetate as the electron donor and 40 mM fumarate as the electron acceptor (Tables S1–S4) under anoxic conditions with a gas phase of N_2/CO_2 (80%/20%) at 30 °C [28]. After 2 days of cultivation, bacteria were centrifuged at 6000 × *g* for 10 min at 4 °C, washed with 0.9% NaCl solution for 3 times, and re-suspended in NBF medium (i.e. NABF medium without acetate) for 12 h to ensure that acetate was exhausted. Thereafter, bacteria were centrifuged, washed and re-suspended in NB medium (i.e. NABF medium without acetate or fumarate), and then used in the subsequent bioreduction experiments.

Conduct of bioreduction experiments

MO solution (1 g/L) was sterilized by filtration with 0.22 μm filters. For the pure-culture experiments, MO with a final concentration of 40 mg/L and dead microalgae with a final cell density of 1.3 × 10^7 cell/mL (i.e. the final chlorophyll concentration of 1.7 mg/L) were added into 20 mL NB medium containing *G. sulfurreducens*. For the mixed-culture experiments, lake water (26° 5′ 29″ N, 119° 14′ 37″ E, Fuzhou, China) at a depth of 2–3 m was collected in January which is not a period of eutrophication with the original chlorophyll concentration being only 1.09 μg/L and the original dissolved oxygen concentration of 3.7 mg/L, and placed in the dark for 12 h to consume the electron donors. Then MO with a final concentration of 1 mg/L and dead microalgae with a final cell density of 3.3 × 10^6 cells/mL (i.e. with a the final chlorophyll concentration of 0.4 mg/L) which was similar to conditions occurring in some natural waters [29, 30] were added into 100 mL of lake water.

Light experiments were conducted with a light-emitting diode (LED) array (light intensity = 2 mW/cm^2, λ = 400–840 nm) illuminating the whole serum bottle, and dark experiments were conducted with the whole serum bottle covered with tin foil. Controls were included that contained: (1) no bacteria; and, (2) no dead microalgae. All treatments were performed under anoxic conditions (N_2:CO_2 = 80:20) at 30 °C with three biological replicates.

The dual-chamber biophotoelectrochemical cell consisted of two cylindrical glass vessels with a liquid volume of 30 mL and a headspace volume of 15 mL, which were separated by a proton exchange membrane (Nafion 117, Dupont, USA) (Fig. S5). Graphite plates (1.5 cm × 1 cm × 0.5 cm) were used as anode and cathode. No external resistance was used during operation. The anode and cathode were connected to each other using titanium wires. The cathode chamber wrapped with tin foil to keep out light was filled with lake water which was not placed in the dark to consume the electron donors before use, and with MO at a final concentration of 1 mg/L. Killed *R. subcapitata* cells were added to the anode chamber to a cell density of 3.3 × 10^6 cells/mL in sterile freshwater medium [31] that was irradiated as described in the LED assay. Both chambers of the bio-photoelectrochemical cell were purged with N_2–CO_2 (80:20) for 30 min before operation to maintain anoxic conditions (i.e. dissolved oxygen concentration <0.5 mg/L).

Detection of MO and decolorization products

Samples were collected from the bottles using disposable sterile syringes and filtered with 0.22 μm filters for MO determination via a spectrometer (UV2600, Shimadzu, Japan) at 465 nm. The MO decolorization efficiency (*R*, %) was calculated as follows [32]:

$$R = \left(1 - C_t/C_0\right) \times 100\% \quad (1)$$

Where C_t is the absorbance at time *t* (h) and C_0 is the initial absorbance at 0 h.

The products of MO decolorization were qualitatively analyzed by gas chromatography mass spectrometry (GCMS-QP2010Utra, SHIMADZU, Japan) and high-performance liquid chromatography (U-3000HPLC, Thermo Fisher Scientific, USA) (see Supporting Information). Concentrations of residual MO and the intermediates of MO decolorization were quantitatively determined using HPLC (E2695, Waters Alliance, USA) according to the previous protocol [33], in which the UV detector was set at 450 nm for MO and 254 nm for N, N-dimethyl-p-phenylenediamine (DPD) and 4-aminobenzenesulfonic acid (4-ABA). The retention times of 4-ABA, DPD and MO were 3.482, 7.783 and 27.637 min, respectively (Fig. S6).

Characterization of dead microalgae

The ultraviolet-visible (UV–Vis) spectra of the concentrated dead microalgae suspension (i.e. dead microalgae suspended in 0.1 M phosphate buffered solution (PBS) with a cell density of 1.3 × 10^7 cell/mL) were recorded using the spectrometer. *I*–*t* curves of dead microalgae were determined using a CHI660E electrochemical workstation (Chenhua Inc., Shanghai, China) via construction of a three electrode system, in which an indium tin oxide (ITP) glass with a size of 1 cm × 2 cm (coated with 200 μL of the concentrated dead microalgae solution) was the working electrode, a saturated calomel electrode (SCE) was the reference electrode, and a platinum wire was the counter electrode [11]. The container was filled 0.1 M PBS and a light-dark mode was applied on the container with the LED array (λ = 400–840 nm). The applied potential was 0.4 V vs SCE. NADPH concentration was used to characterize the activity of the intracellular ferredoxin-NADP$^+$-reductase and was measured with the Solarbio Coenzyme II NADP(H) Content Assay Kit (BC1100).

The gas chromatography mass spectrometry (GC-MS, 8890-5977B, Agilent, USA) and the ultra-performance liquid chromatography-tandem mass spectrometry (UPLC-MS/MS, UPLC: ExionLC AD, SCIEX, Japan; MS/MS: QTRAP6500+ System, SCIEX, Japan) were used to detect the organic carbon produced by decomposition of the dead microalgae (see Supporting Information).

Microbial analysis

For the pure-culture experiment, after a 4-h operation, total RNA was extracted and reverse-transcribed using a RNeasy Mini Kit. The primers of reverse transcription quantitative real-time PCR (RT-qPCR) were employed to quantify the abundance of the cytochrome OmcS, OmcZ and OmcB, the structural pilin protein PilA and housekeeping protein RecA gene transcripts in *G. sulfurreducens* using the LightCycler 96 System (Roche, Mannheim, Germany). The primers used for these genes (Table S5) were constructed according to previous studies [34, 35]. The reactions were carried out in a final volume of 20 μL containing 5 μL RNA samples and the amplification program was set according to the previously described method [22].

For the mixed-culture bioreduction experiment in serum bottles, after a 32-h operation, the total DNA of microbial communities in the water was extracted using the Power-Soil DNA Isolation Kit (MoBio Laboratories Inc., Carlsbad, USA) and quantified with a NanoDrop spectrophotometer (ND2000, Gene Co. Ltd, Australia). Universal primers 515F and 909R [36] were used to amplify the V4–V5 hypervariable region of the 16S rRNA gene. The PCR mixture (25 μL) contained a 1×Taq Plus Master Mix, 6 ng BSA, each primer was present at 1.0 μM and 30 ng DNA. The PCR amplification program included an initial denaturation step at 94 °C for 5 min, followed by 30 cycles at 94 °C for 30 s, 55 °C 30 s, and 72 °C for 60 s, and a final extension step at 72 °C for 7 min. The PCR products were purified using an Agencourt AMPure

XP Kit and sequenced using a MiSeq System (Allwegene Company, Beijing, China). The raw reads were demultiplexed, combined, quality filtered, de-replicated and chimeras removed using QIIME2 (Version 2020.8) and denoised into amplicon sequence variants (ASVs) using the DADA2 as the plugin in QIIME2 [37, 38]. The ASVs were processed with the Ribosomal Data Project classifier (Version 18, https://rdp.cme.msu.edu) [39]. The sequence raw data reported in this study were submitted to the NCBI Sequence Read Archive (http://www.ncbi.nlm.nih.gov/sra) with the accession numbers SRR23217474-SRR23217485 under the BioProject PRJNA925680.

Data analysis

All of the tests were performed in triplicate unless otherwise noted, and the mean values were reported. Data were available at Zenodo (doi: 10.5281/zenodo.7553088). The software Origin 8.5 was used to draw figures. One-way analysis of variance (ANOVA) followed by the least significant difference test ($p < 0.05$) (SPSS statistical software Version 21.0) was used to complete statistical analyses.

RESULTS AND DISCUSSION

Dead *Raphidocelis* and live *Geobacter* co-drive the anaerobic reduction process

The dead *R. subcapitata*–live *G. sulfurreducens* experiment and a series of deletional control experiments were conducted. The MO decolorization reached 97% within 8 h in the presence of dead microalgae, live bacteria and light corresponding to a zero-order reaction with a kinetic constant of 0.12 ($R^2 = 0.997$) (Fig. 1A). In contrast, the MO decolorization in the dark control (Fig. 1B) or the no-microalgal control were only 25–29% within 8 h, and the dead bacterial control had almost no decolorization whether performed under dark or light irradiation conditions.

MO might have been decolorized by the following 2 pathways: (1) oxidation via asymmetric cleavage of the N–C bond; [40] or (2) reduction via azo-bond (N=N) cleavage [41, 42]. Analysis of the decolorization products of MO in the dead *R. subcapitata*–live *G. sulfurreducens* under light irradiation revealed that the major final products were DPD and 4-ABA (Figs. S7 and S8). DPD and 4-ABA are typical products of MO reduction [43, 44], and their final concentrations in this group accounted for ~88% and ~91% of the concentration of MO decolorization, respectively (Fig. S9A), indicating most of MO in our experiment was decolorized by reduction but not by absorption or oxidation.

Percentages of MO decolorization in the control groups were close to those reported in the previous study [45]. Most of the MO decolorization in the dark control and the no-microalgal control also resulted from MO reduction, since the DPD and 4-ABA concentrations in these control groups accounted for ~80% and ~84% of the concentrations of MO decolorization, respectively (Figs. S8B and S9A). MO reduction in these control groups could be attributed to the electron storage capacity of cytochromes in *G. sulfurreducens* which were able to store approximately 10^7 electrons per cell [46, 47]. These stored electrons were able to be discharged to electron acceptors in a subsequent process when the live cells were transferred to a medium with abundant electron acceptors [48, 49]. Under the dark condition, MO reduction in the group with dead algae addition was lower than that in the no dead algae group. The reason for this result might be that there were some reactive oxide species in the apoptotic microalgae cells [50, 51] which would consume parts of the stored electrons in cytochromes in *G. sulfurreducens*.

Light intensities in different water bodies such as lake, reservoir and rice field ranged from 0.01–600 μE/m^2 s [52–54], thus the effects of different light intensities were studied. The *I–t* curves with light intensities from 0.2 mW/cm^2 to 20 mW/cm^2 were compared (Fig. S10A). The higher the light intensity, the higher the photocurrent. The dead *R. subcapitata*–live *G. sulfurreducens* experiment with light intensities from 0.2 mW/cm^2 to 20 mW/cm^2 were able to promote the MO reduction (Fig. S10B). The higher the light intensity, the faster the MO reduction.

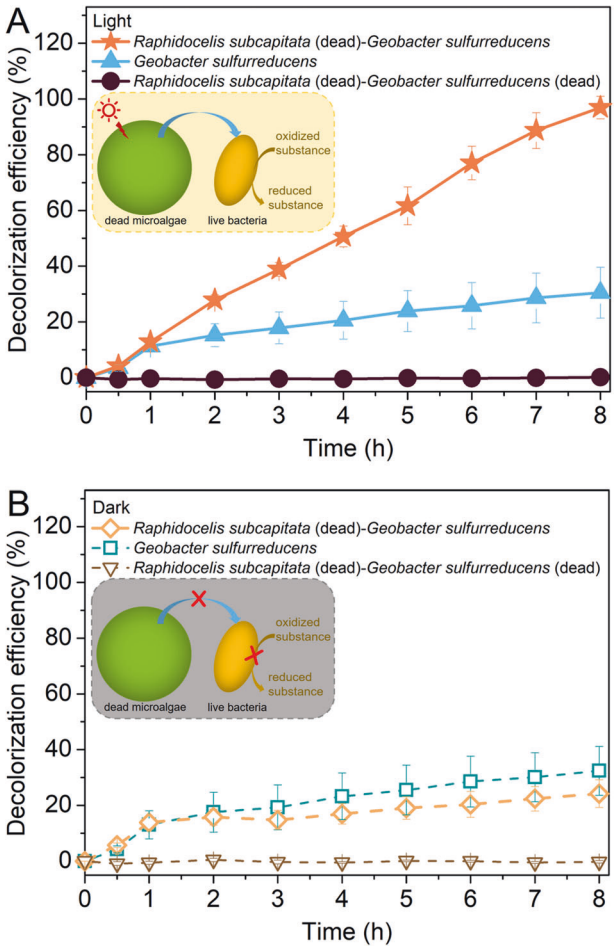

Fig. 1 Anaerobic reduction process co-driven by dead *Raphidocelis subcapitata* and live *Geobacter sulfurreducens*. Time curves of methyl orange decolorization by dead *Raphidocelis subcapitata* and live *Geobacter sulfurreducens* and control experiments in serum bottles (**A**) in the light and (**B**) in the dark. Results are the mean and standard deviation for triplicate cultures.

Photoelectric mechanisms between dead *Raphidocelis subcapitata* and live *Geobacter sulfurreducens*

The UV–Vis spectrum of microalgae solution shows that both dead and live *R. subcapitata* absorbed at wavelengths of 300–700 nm with several significant peaks at approximately 430, 490, 625 and 675 nm (Fig. 2A), similar to those of chlorophyll a and lutein [55, 56]. The *I–t* curve demonstrated that dead microalgae generated photocurrent (~0.08 μA/cm^2) upon irradiation while the live microalgae generated no measureable current (Fig. 2B and S3). The pigment activity in dead microalgae cells had been reported in the previous study [57]. The *I–t* curves of dead *R. subcapitata* with a cell density of 1.3 × 10^7 cell/mL and pure chlorophyll a (C805046, purchased from Macklin) with the concentration of 1.7 mg/L (i.e. the equal chlorophyll concentration to that in the 1.3 × 10^7 cell/mL of dead *R. subcapitata*) are compared in Fig. S11. Results showed that the photocurrents produced by the dead microalgae cells were close to those produced by equal amounts of chlorophyll a, suggesting that the photocurrents generated by the dead microalgae cells mainly resulted from active pigments. Photocurrent produced by dead microalgae was lower but more stable than an easy-corrosive semiconductor such as CdS [11].

The chlorophyll concentrations in different water bodies ranged from 0.001–5 mg/L [58, 59], thus effects of different dead microalgae cell densities (i.e. different chlorophyll concentrations) were studied. The *I–t* curves with dead microalgae cell densities

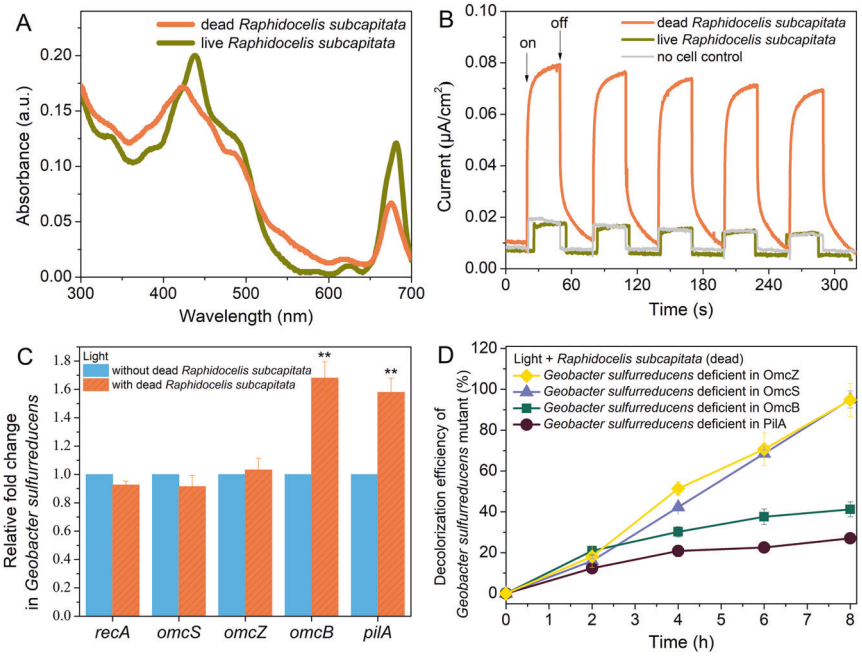

Fig. 2 Photoelectric mechanisms in the dead *Raphidocelis subcapitata*–live *Geobacter sulfurreducens* experiment. A UV–vis spectra of dead *Raphidocelis subcapitata* solution. **B** *I–t* curve of the dead *Raphidocelis subcapitata*-coated ITO glass electrode in a light-dark cyclic experiment. **C** Relative transcript abundance of genes in *Geobacter sulfurreducens*. Asterisks represent a significant difference (**$p < 0.05$) from the control without dead microalgae. **D** Time curves of methyl orange decolorization by dead *Raphidocelis subcapitata* and live *Geobacter sulfurreducens* mutants in light. Data represent average values for triplicate samples.

from 1.3×10^5 cell/mL to 3.9×10^7 cell/mL (i.e. chlorophyll concentrations from 0.017 mg/L to 5 mg/L) were compared (Fig. S12A). The higher the dead microalgae cell density, the higher the photocurrent. The dead *R. subcapitata*–live *G. sulfurreducens* experiment with dead microalgae cell densities ranging from 1.3×10^5 cell/mL to 3.9×10^7 cell/mL could promote MO reduction (Fig. S12B). The higher the microalgae cell densities (i.e. chlorophyll concentrations), the faster the MO reduction.

The live microalgae were also able to absorb light energy but could not output photocurrent (Fig. 2A, B). This result occurred since the dominant acceptor of the photoelectrons produced by active pigments in live microalgae cells is the intracellular electron transport chain associated with photosynthesis, i.e. the reaction $NADP^+ + 2e^- + H^+ \xrightarrow{FNR} NADPH$, which is catalyzed by the intracellular ferredoxin-$NADP^+$-reductase (FNR) in the live microalgae [60]. If this pathway is still operating, the photoelectrons will end inside the microalgae cells, thus photocurrents will not be able to be detected using the electrochemical workstation. If this pathway is inactivated, the photoelectrons are able to transfer to the extracellular environment and we can detect them. To confirm this inference, we used the content of NADPH to indicate whether the intracellular electron transport chain associated with photosynthesis is inactivated [61]. That is, lower contents of NADPH indicated that the intracellular electron transport chain and FNR were less activated. In the dead microalgae, no matter what inactivation methods were used, the intracellular electron transport chain did not work as well as it did in the live microalgae (Fig. S4), thus the photoelectrons generated by the active pigments are able to transfer to the extracellular electron acceptors. When less photoelectrons transfer to the intracellular electron transport chain, more photoelectrons will transfer to the extracellular environment then to be detected. Therefore, the NADPH contents and the photoelectrons we detected were negatively correlated (Figs. S3 and S4). More detected photoelectrons led to better MO reduction performance. For example, the 121 °C-inactivated dead microalgae cells which had a lower NADPH content and higher photocurrent resulted in faster MO reduction than the 65 °C-inactivated dead microalgae cells (Fig. S13).

In order to investigate whether the organic carbon generated by decomposition of the dead microalgae acted as carbon sources for bacteria and then led to a higher reduction efficiency of MO, organic carbon products after decomposition both under dark and light conditions were identified and quantified. Concentrations of nine types of acids and two types of saccharides were slightly higher under the light condition than they were in the dark (Fig. S14A, B). However, *G. sulfurreducens* is not able to use any of these organic carbon products as electron donors [62], demonstrating that organic carbon products produced by decomposition of the dead microalgae did not act as carbon sources in the pure-culture experiment with *G. sulfurreducens*.

Under light irradiation, *G. sulfurreducens* with dead *R. subcapitata* addition in the serum bottle experiment had a higher transcript abundance (1.7-fold, $p < 0.05$) of the *omcB* gene encoding OmcB that is associated with the outer cell surface, and higher levels of transcription (1.6 fold, $p < 0.05$) of the *pilA* gene encoding a structural pilin protein of the type IV pili compared to those genes without dead microalgae (Fig. 2C). OmcB is able to mediate heterogeneous electron transfer between microorganisms and extracellular electron donors/acceptors, and the type IV pilus has been implicated in long-distance electron transfer [63–65]. The higher rate of transcription of the *omcB* and the *pilA* genes with dead *R. subcapitata* addition suggested that both the OmcB cytochrome and the type IV pili play important roles in the illuminated dead *R. subcapitata*–live *G. sulfurreducens* interaction. Mutants were used to further confirm this mechanism. The PilA-deficient mutant we used was the pili mutant which also affects the extracellular OmcS [23]. Both the OmcB-deficient mutant and the PilA-deficient mutant displayed much lower MO reduction, while the OmcZ-deficient mutant and the OmcS-deficient mutant displayed slightly lower MO reduction efficiencies only within the first 2 to 4 h compared to the wild-type strain

and then the three strains displayed no significant differences (Figs. 2D, S9B and Table S6), demonstrating that efficient electron transport required both the OmcB cytochromes and the type IV pili in the illuminated dead *R. subcapitata*–live *G. sulfurreducens* experiment. MO reductions of the OmcB-deficient mutant and the PilA-deficient mutant were close to those obtained in the control groups (Fig. 1A, B) which were also attributed to the electron storage capacity of cytochromes.

These results strongly suggest that the illuminated dead microalgal cells were able to act as the microbial photosensitizer to significantly improve the rate and extent of anaerobic reduction in living *G. sulfurreducesn* cells. Direct evidence showed that the improvement is not a result of the organic carbon provided by decomposition of the dead microalgae, and could be attributed to the outward flow of photoelectrons from the still-functional pigments of the dead microalgae.

Dead microalgae as microbial photosensitizer drive the anaerobic bioreduction process in lake water

To investigate whether the photoelectric mechanism of dead microalgae is also able to work in the complicated aqueous mixed-bacteria environment, lake water of the non-trophic period was collected to set up the serum bottle and the biophotoelectrochemical-cell experiments with dead microalgae addition. After 12 h in the dark for electron donor extinction, the lake water could hardly decolorize MO (i.e. below 6%) (Fig. 3A). However, in the presence of dead *R. subcapitata*, the MO decolorization efficiency in lake water increased no matter whether under dark (49 ± 9%) or illuminated conditions (97 ± 1%) within 20 h. If the lake water was sterilized, the dead microalgae addition was not able to decolorize MO. These results demonstrated that dead microalgae enhanced the decolorization efficiency in a mixed-bacteria environment. Based on the metabolome data (Fig. 2C, D), the increase in MO decolorization by dead microalgae addition in the dark might be caused by organic nutrient substances produced by decomposition of dead microalgae acting as electron donors, which is consistent with previous studies [3, 8].

The bioreduction efficiencies in light were twice of that in the dark (Fig. 3A) while the types and total content of decomposition products of dead algae under light and under dark conditions were similar (organic acids: 67.4 μg/L (light) vs. 66.2 μg/L (dark); saccharide: 158.9 μg/L (light) vs. 159.6 μg/L (dark)) (Fig. 2C, D), suggesting that dead microalgae might also act as microbial photosensitizers in lake water.

Microbial communities in lake water under different treatments were analyzed to provide bacterial evidence for the above-suggested mechanisms. Some bacteria belonging to *Aquitalea* sp., *Pelosinus* sp., and *Prevotella* sp. have been shown to be capable of degrading celluloses and saccharides, among which *Aeromonas* sp. and *Clostridium* sp. have been shown to reduce MO [66–69]. The relative abundances of all bacterial genera that are able to utilize celluloses and saccharides as their carbon sources for growth were illustrated in Fig. 4A. These types of bacteria increased after addition of dead microalgae both in the dark and in the light. Thus, celluloses and saccharides produced by decomposition of dead microalgae were probably correlated to the increase in bioreduction in the dark group and partial enhancement of bioreduction in the light group (Fig. 3A, B). All bacteria capable of utilizing photoelectrons belong to electroactive microorganisms [14–16, 70, 71]. The abundance of electroactive bacteria in the illuminated group with dead microalgae addition was significantly higher than the abundance of other groups, especially the *Geobacter* sp., *Rhodopseudomonas* sp. and *Tolumonas* sp. compared to the dark group with dead microalgae addition (Fig. 4B).

Biophotoelectrochemical cells were set up to physically separate the dead microalgae and live bacteria in lake water so

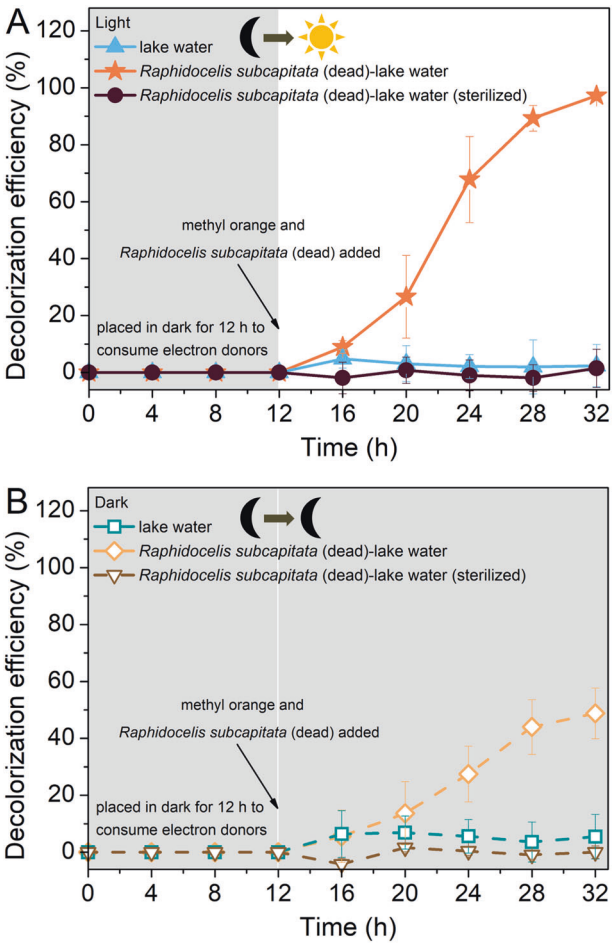

Fig. 3 Anaerobic reduction process co-driven by dead microalgae and live mixed-bacteria in lake water. Time curves of methyl orange reduction in lake water with dead *Raphidocelis subcapitata* and control experiments in serum bottles (**A**) in the light and (**B**) in the dark. Results are the mean and standard deviation for triplicate cultures.

that only electrons are able to transfer from the dead microalgae-anode to the live bacteria-cathode but that the nutrient substance from microalgae decomposition cannot. The dead microalgae-anode under light irradiation led to significantly higher MO reduction by lake water in the cathode chamber than in the control groups (Fig. 4C). This difference was almost equal to the difference in MO reduction efficiencies with dead microalgae between the dark and the light conditions in Figs. 3A, B, demonstrating that the main reason for promotion of MO reduction under irradiation by dead microalgae was the photoelectrons but not the nutrient substances provided by the microalgae. Biophotoelectrochemical cells with a fixed external resistance of 1000 Ω were constructed and demonstrated that there were indeed electrons transferred from the dead microalgae-anode to the live bacteria-cathode under light irradiation (Fig. S15). Therefore, the photoelectric mechanism of dead microalgae is indeed operating in the complicated aqueous mixed-bacteria environment, revealing a new pathway providing a synergistic linkage between microalgae and bacteria. In addition, some electron shuttles such as anthraquinone-2-sulfonate and biochar were able to promote the photoelectrotrophic linkage between dead microalgae and live bacteria in the complicated aqueous mixed-bacteria environment (Fig. S16).

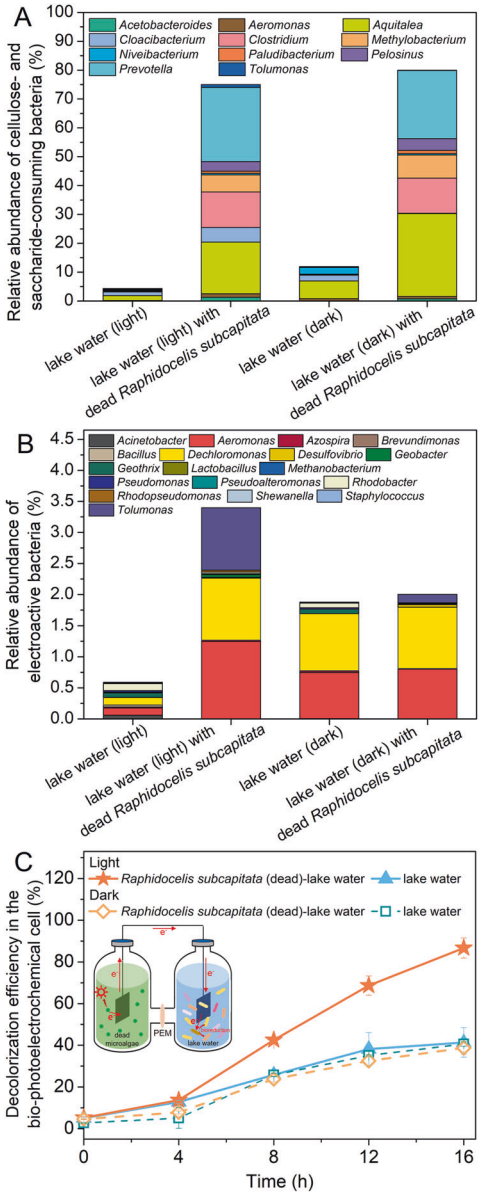

Fig. 4 Evidences for a biophotoelectrochemical process in a mixed-bacteria environment. A cellulose- and saccharide-consuming bacteria and **B** typical electroactive bacteria at the genus level in lake water with dead *Raphidocelis subcapitata* and control experiments in serum bottles. **C** Time curves of methyl orange reduction in lake water in bio-photoelectrochemical cells. Data represent average values for triplicate samples.

CONCLUSION

In summary, the present study demonstrates that irradiated dead microalgal cells are able to act as microbial photosensitizers to drive anaerobic bioreduction by EET-capable bacteria, suggesting a photoelectrotrophic linkage between irradiated microalgae and live EET-capable bacteria. In addition to the MO reduction used as the model anaerobic reduction process in this work, other biogeochemical processes such as carbon/nitrogen fixation, nitrate reduction and metal reduction that can be driven by photoelectrons and electroactive bacteria, can also be driven by the photoelectric effect between dead microalgae and live bacteria (Fig. 5). For example, NO_3^- reduction can be driven by dead *Chlorella vulgaris* and live *Shewanella oneidensis* (Fig. S17A), and Cr(VI) reduction can be driven by dead *Raphidocelis subcapitata* and live *Bacillus subtilis* (Fig. S17B). Thus the discovery of this light-triggered mechanism is predicted to provide a new understanding for the algal-bacterial interactions and some biogeochemical process in eutrophic waters. In addition, our results showed that this photoelectric synergistic linkage is able to facilitate the enrichment and growth of EET-capable bacteria, and modulate the microbial community to acclimate to the surrounding environment, which has ecological significance in nature.

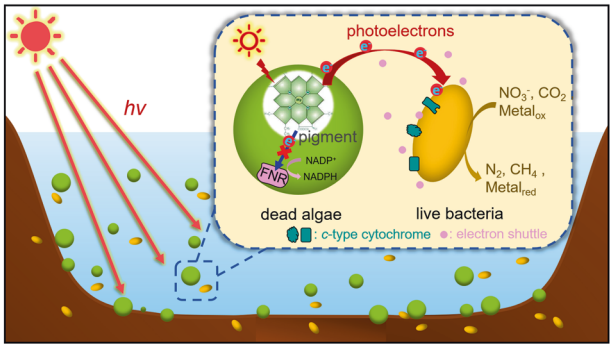

Fig. 5 Proposed photoelectric mechanism of the anaerobic reduction process co-driven by dead microalgae and live bacteria. Photoelectrons generated from the illuminated dead microalgae stem from the pigments of dead microalgae staying active while the ferredoxin-$NADP^+$-reductase (FNR) becoming inactivated. photoelectrons are transferred to the live bacteria capable of extracellular electron transfer through multiheme cytochromes or electron shuttles, and then drive some anaerobic reduction processes.

Furthermore, the anaerobic reduction process co-driven by photoelectric effects between dead microalgae and live bacteria stems from the pigments of dead microalgae staying active while the FNR becomes inactivated. Photosynthetic pigments are essential for photosynthesis of plants, algae bacteria and archaea. The death and decomposition of photosynthetic organisms bring a wide array and abundance of photosynthetic pigments into surface water, sediment and soil. Therefore, this study will also deepen our understanding of the relationships between bacteria and other photosynthetic organisms in the natural environment and will inspire the exploration of similar synergistic linkages between EET-capable microorganisms and photosynthetic bacteria/plants in future studies.

DATA AVAILABILITY

The DNA sequence raw data have been deposited in the NCBI Sequence Read Archive (http://www.ncbi.nlm.nih.gov/sra) with the accession numbers SRR23217474-SRR23217485 under the BioProject PRJNA925680. All other data are available at Zenodo (https://doi.org/10.5281/zenodo.7553088).

REFERENCES

1. Maúre ER, Terauchi G, Ishizaka J, Clinton N, DeWitt M. Globally consistent assessment of coastal eutrophication. Nat Commun. 2021;12:6142.
2. Paerl H, Gardner W, McCarthy M, Peierls B, Wilhelm S. Algal blooms: noteworthy nitrogen. Science. 2014;346:175.
3. Zhu L, Shi W, Van Dam B, Kong L, Yu J, Qin B. Algal accumulation decreases sediment nitrogen removal by uncoupling nitrification-denitrification in shallow eutrophic lakes. Environ Sci Technol. 2020;54:6194–201.
4. Wang P, Laws E, Wang Y, Chen J, Song X, Huang R, et al. Elevated pCO2 changes community structure and function by affecting phytoplankton group-specific mortality. Mar Pollut Bull. 2022;175:113362.
5. Yang J, Holbach A, Wilhelms A, Krieg J, Qin Y, Zheng B, et al. Identifying spatio-temporal dynamics of trace metals in shallow eutrophic lakes on the basis of a case study in Lake Taihu, China. Environ Pollut. 2020;264:114802.
6. Liang X, Zhang X, Sun Q, He C, Chen X, Liu X, et al. The role of filamentous algae *Spirogyra* spp. in methane production and emissions in streams. Aquat Sci. 2016;78:227–39.
7. Shen Y, Huang Y, Hu J, Li P, Zhang C, Li L, et al. The nitrogen reduction in eutrophic water column driven by *Microcystis* blooms. J Hazard Mater. 2020;385:121578.

8. Chen X, Huang Y, Chen G, Li P, Shen Y, Davis TW. The secretion of organics by living *Microcystis* under the dark/anoxic condition and its enhancing effect on nitrate removal. Chemosphere. 2018;196:280–7.
9. Lu A, Li Y, Jin S, Wang X, Wu X, Zeng C, et al. Growth of non-phototrophic microorganisms using solar energy through mineral photocatalysis. Nat Commun. 2012;3:768.
10. Li Y, Li Y, Liu Y, Wu Y, Wu J, Wang B, et al. Photoreduction of inorganic carbon (+V) by elecmental sulfur: implications for prebiotic synthesis in terrestrial hot springs. Sci Adv. 2020;6:eabc3687.
11. Huang S, Chen M, Dian Y, Feng Q, Zeng RJ, Zhou S. Dissolved organic matter acting as a microbial photosensitizer drives photoelectrophic denitrification. Environ Sci Technol. 2022;56:4632–41.
12. Chen M, Cai Q, Chen X, Huang S, Feng Q, Majima T, et al. Anthraquinone-2-sulfonate as a microbial photosensitizer and capacitor drives solar-to-N_2O production with a quantum efficiency of almost unity. Environ Sci Technol. 2022; 56:5161–9.
13. Sakimoto KK, Wong AB, Yang P. Self-photosensitization of nonphotosynthetic bacteria for solar-to-chemical production. Science. 2016;351:74–77.
14. Ye J, Yu J, Zhang Y, Chen M, Liu X, Zhou S, et al. Light-driven carbon dioxide reduction to methane by *Methanosarcina barkeri*-CdS biohybrid. Appl Catal B Environ. 2019;257:117916.
15. Chen M, Zhou X, Yu Y, Liu X, Zeng RJ, Zhou S, et al. Light-driven nitrous oxide production via autotrophic denitrification by self-photosensitized *Thiobacillus denitrificans*. Environ Int. 2019;127:353–60.
16. Cestellos-Blanco S, Zhang H, Kim JM, Shen Y, Yang P. Photosynthetic semiconductor biohybrids for solar-driven biocatalysis. Nat Catal. 2020;3:245–55.
17. Huang L, Liu X, Zhang Z, Ye J, Rensing C, Zhou S, et al. Light-driven carbon dioxide reduction to methane by *Methanosarcina barkeri* in an electric syntrophic coculture. ISME J. 2022;16:370–7.
18. Ding R, Yan W, Wu Y, Xiao Y, Gang H, Wang S, et al. Light-excited photoelectrons coupled with bio-photocatalysis enhanced the degradation efficiency of oxytetracycline. Water Res. 2018;143:589–98.
19. Ren G, Yan Y, Nie Y, Lu A, Wu X, Li Y, et al. Natural extracellular electron transfer between semiconducting minerals and electroactive bacteria communities occurred on the rock varnish. Front Microbiol. 2019;10:293.
20. Luo L, Wang P, Lin L, Luan T, Ke L, Tam NFY. Removal and transformation of high molecular weight polycyclic aromatic hydrocarbons in water by live and dead microalgae. Process Biochem. 2014;49:1723–32.
21. Luo L, Xiao Z, Chen B, Cai F, Fang L, Lin L, et al. Natural porphyrins accelerating the phototransformation of Benzo[a]pyrene in water. Environ Sci Technol. 2019;52:3634–41.
22. Chen S, Deng C, Liu X, Yang Y, Cai X, Huang H, et al. CdS nanoparticles alleviate photo-induced stress in *Geobacter* co-cultures. Environ Sci Nano. 2019;6:1941–9.
23. Liu X, Zhuo S, Rensing C, Zhou S. Syntrophic growth with direct interspecies electron transfer between pili-free *Geobacter* species. ISME J. 2018;12:2142–51.
24. Huang S, Tang J, Liu X, Dong G, Zhou S. Fast light-driven biodecolorization by a *Geobacter sulfurreducens*-CdS biohybrid. ACS sustain. Chem Eng. 2019;7:15427–33.
25. Zhu L, Wang Z, Shu Q, Takala J, Hiltunen E, Feng P, et al. Nutrient removal and biodiesel production by integration of freshwater algae cultivation with piggery wastewater treatment. Water Res. 2013;47:4294–302.
26. Machado MD, Soares EV. Development of a short-term assay based on the evaluation of the plasma membrane integrity of the alga *Pseudokirchneriella subcapitata*. Appl Microbiol Biotechnol. 2012;95:1035–42.
27. Ye Y, Liu X, Nealson KH, Rensing C, Qin S, Zhou S. Dissecting the structural and conductive functions of nanowires in *Geobacter sulfurreducens* electroactive biofilms. mBio. 2022;13:e03822–21.
28. Coppi MV, Leang C, Sandler SJ, Lovley DR. Development of a genetic system for *Geobacter sulfurreducens*. Appl Environ Microbiol. 2001;67:3180–7.
29. Backer LC, McNeel SV, Barber R, Kirkpatrick B, Williams C, Irvin M, et al. Recreational exposure to microcystins during algal blooms in two California lakes. Toxicon. 2010;55:909–21.
30. Oudra B, Loudiki M, Sbiyyaa B, Martins R, Vasconcelos V, Namikoshi N. Isolation, characterization and quantification of microcystins (heptapeptides hepatotoxins) in *Microcystis aeruginosa* dominated bloom of Lalla Takerkoust lake-reservoir (Morocco). Toxicon. 2001;39:1375–81.
31. Nevin KP, Kim BC, Glaven RH, Johnson JP, Woodard TL, Methe BA, et al. Anode biofilm transcriptomics reveals outer surface components essential for high density current production in *Geobacter sulfurreducens* fuel cells. PLoS ONE. 2009;4:e5628.
32. Fang Y, Xu M, Wu W, Chen X, Sun G, Guo J, et al. Characterization of the enhancement of zero valent iron on microbial azo reduction. BMC Microbiol. 2015;15:85–93.
33. Shen N, Huo Y, Chen J, Zhang F, Zheng H, Zeng RJ. Decolorization by *Caldicellulosiruptor saccharolyticus* with dissolved hydrogen under extreme thermophilic conditions. Chem Eng J 2015;262:847–53.
34. Liu F, Rotaru AE, Shrestha PM, Malvankar NS, Nevin KP, Lovley DR. Magnetite compensates for the lack of a pilin-associated *c*-type cytochrome in extracellular electron exchange. Environ Microbiol. 2015;17:648–55.
35. Leang C, Coppi MV, Lovley DR. OmcB, a c-type polyheme cytochrome, involved in Fe(III) reduction in *Geobacter sulfurreducens*. J Bacteriol. 2003;185:2096–103.
36. Chen S, Yang Y, Jing X, Zhang L, Chen J, Rensing C, et al. Enhanced aging of polystyrene microplastics in sediments under alternating anoxic-oxic conditions. Water Res. 2021;207:117782.
37. Callahan BJ, McMurdie PJ, Rosen MJ, Han AW, Johnson AJA, Holmes SP. DADA2: high-resolution sample inference from illumina amplicon data. Nat Methods. 2016;13:581–3.
38. Callahan BJ, Wong J, Heiner C, Oh S, Theriot CM, Gulati AS, et al. High-throughput amplicon sequencing of the full-length 16S rRNA gene with single-nucleotide resolution. Nucleic Acids Res. 2019;47:103.
39. Edgar RC. UPARSE: highly accurate OTU sequences from microbial amplicon reads. Nat Methods. 2013;10:996.
40. Mishra A, Kumar S, Pandey AK. Laccase production and simultaneous decolorization of synthetic dyes in unique inexpensive medium by new isolates of white rot fungus. Int Biodeter Biodegr. 2011;65:487–93.
41. Cai P, Xiao X, He Y, Li W, Chu J, Wu C, et al. Anaerobic biodecolorization mechanism of methyl orange by *Shewamella oneidensis* MR-1. Appl Microbiol Biot. 2012;93:1769–76.
42. Liu Y, Zhang F, Li J, Li D, Liu D, Li W, et al. Exclusive extracellular bioreduction of methyl orange by azo reductase-free *Geobacter sulfurreducens*. Environ Sci Technol. 2017;51:8616–23.
43. Wang Q, Huang L, Quan X, Puma GL. Sequential anaerobic and electro-Fenton processes mediated by W aLnd Mo oxides for degradation/mineralization of azo dye methyl orange in photo assisted microbial fuel cells. Appl Catal B-Environ. 2019;245:672–80.
44. Zhao H, Huang S, Xu W, Wang Y, Wang Y, He C, et al. Undiscovered mechanism for pyrogenic carbonaceous matter-mediated abiotic transformation of azo dyes by sulfide. Environ Sci Technol. 2019;53:4397–405.
45. Huang S, Tang J, Liu X, Dong G, Zhou S. Fast light-driven biodecolorization by a *Geobacter sulfurreducens*-CdS biohybrid. ACS Sustain Chem Eng. 2019;7: 15427–33.
46. Esteve-Nunez A, Sosnik J, Visconti P, Lovley DR. Fluorescent properties of c-type cytochromes reveal their potential role as an extracytoplasmic electron sink in *Geobacter sulfurreducens*. Environ Microbiol. 2008;10:497–505.
47. Malvankar SN, Mester T, Tuominen TM, Lovley RD. Supercapacitors based on c-type cytochromes using conductive nanostructured networks of living bacteria. Chemphyschem. 2012;13:463–8.
48. Lovley DR, Ueki T, Zhang T, Malvankar NS, Shrestha PM, Flanagan KA, et al. *Geobacter*: the microbe electric's physiology, ecology, and practical applications. Adv Micro Physiol. 2011;59:1–100.
49. Bonanni PS, Schrott GD, Robuschi L, Busalmen JP. Charge accumulation and electron transfer kinetics in *Geobacter sulfurreducens* biofilms. Energy Environ Sci. 2012;5:6188–95.
50. Segovia M, Berges JA. Inhibition of caspase-like activities prevents the appearance of reactive oxygen species and dark-induced apoptosis in the unicellular chlorophyte *Dunaliella tertiolecta*. J Phycol. 2009;45:1116–26.
51. Zhu Y, Zhong X, Wang Y, Zhao Q, Huang H. Growth performance and antioxidative response of *Chlorella pyrenoidesa*, *Dunaliella salina*, and *Anabaena cylindrica* to four kinds of ionic liquids. Appl Biochem Biotechnol 2021;193: 1945–66.
52. Zhang J, Shu X, Zhang Y, Tan X, Zhang Q. The responses of epilithic algal community structure and function to light and nutrients and their linkages in subtropical rivers. Hydrobiologia. 2020;847:841–55.
53. Murakami T, Terai H, Yoshiyama Y, Tezuka T, Zhu L, Matsunaka T, et al. The second investigation of Lake Puma Yum Co located in the southern Tibetan Plateau, China. Limnology. 2007;8:331–5.
54. Gao J, Zhu J, Wang M, Dong W. Dominance and growth factors of *Pseudanabaena* sp. in drinking water source reservoirs, southern China. Sustainability. 2018;10:1–15.
55. Ferreira A, Stramski D, Garcia CAE, Garcia VMT, Ciotti AM, Mendes CRB. Variability in light absorption and scattering of phytoplankton in Patagonian waters: role of community size structure and pigment composition. J Geophys Res Oceans. 2013;118:698–714.
56. Quaranta A, Krieger-Liszkay A, Pascal AA, Perreau F, Robert B, Vengris M, et al. Singlet fission in naturally-organized carotenoid molecules. Phys Chem Chem Phys. 2021;23:4768–76.
57. Luo L, Lai X, Chen B, Lin L, Fang L, Tam NFY, et al. Chlorophyll catalyse the phototransformation of carcinogenic benzo[a]pyrene in water. Sci Rep. 2015;5:12776.
58. Mineeva NM. Content of photosynthetic pigments in the upper volga reservoirs (2005-2016). Inland Water Biol. 2019;12:161–9.

59. Mathanmohun M, Ramasamy S, Krishnamoorthy S, Palve AM, Palanisamy A. Screening, molecular detection and hydrocarbon investigation of microalgae from paddy fields of Rasipuram area, Namakkal, Tamil Nadu. Mater Today Proc. 2021;47:440–5.
60. Rumpel S, Siebel JF, Fares C, Duan JF, Reijerse E, Happe T, et al. Enhancing hydrogen production of microalgae by redirecting electrons from photosystem I to hydrogenase. Energ Environ Sci. 2014;7:3296–301.
61. Lendzian K, Bassham JA. NADPH/$NADP^+$ ratios in photosynthesizing reconstituted chloroplasts. Biochim Biophys Acta. 1976;430:478–89.
62. Caccavo FJ, Lonergan DJ, Lovley DR, Davis M, Stolz JF, McInerney MJ. *Geobacter sulfurreducens* sp. nov., a hydrogen- and acetate-oxidizing dissimilarity metal-reducing microorganism. Appl Environ Microbiol. 1994;60:3752–9.
63. Richter H, Nevin KP, Jia H, Lowy DA, Lovley DR, Tender LM. Cyclic voltammetry of biofilms of wild type and mutant *Geobacter sulfurreducens* on fuel cell anodes indicates possible roles of OmcB, OmcZ, type IV pili, and protons in extracellular electron transfer. Energy Environ Sci. 2009;2:506–16.
64. Liu X, Zhan J, Jing X, Zhou S, Lovley DR. A pilin chaperone required for the expression of electrically conductive *Geobacter sulfurreducens* pili. Environ Microbiol. 2019;21:2511–22.
65. Walker DJF, Adhikari RY, Holmes DE, Ward JE, Woodard TL, Nevin KP, et al. Electrically conductive pili from pilin genes of phylogenetically diverse microorganisms. ISME J. 2018;12:48–58.
66. Pan Y, Zheng X, Xiang Y. Structure-function elucidation of a microbial consortium in degrading rice straw and producing acetic and butyric acids via metagenome combining 16S rDNA sequencing. Bioresour Technol. 2021;340:125709.
67. Pankratov TA, Ivanova AO, Dedysh SN, Liesack W. Bacterial populations and environmental factors controlling cellulose degradation in an acidic *Sphagnum* peat. Environ Microbiol. 2011;13:1800–14.
68. Cui J, Mai G, Wang Z, Liu Q, Zhou Y, Ma Y, et al. Metagenomic insights into a cellulose-rich niche reveal microbial cooperation in cellulose degradation. Front Microbiol. 2019;10:618.
69. Chun J, Kang JY, Jung YC, Jahng KY. *Niveibacterium umoris* gen. nov., sp. nov., isolated from wetland freshwater. Int J Syst Evol Microbiol. 2016;66:997–1002.
70. Koch C, Harnisch F. Is there a specific ecological niche for electroactive microorganisms? ChemElectroChem 2016;3:1282–95.
71. Logan BE, Rossi R, Ragab A, Saikaly PE. Electroactive microorganisms in bioelectrochemical systems. Nat Rev Microbiol. 2019;17:307–19.

ACKNOWLEDGEMENTS

This work was financially supported by the National Natural Science Foundation of China (92251301 and 42277101), and the Program for Guangdong Introducing Innovative and Entrepreneurial Teams (2019ZT08L213).

AUTHOR CONTRIBUTIONS

SC designed the experiments, conducted analyses and wrote the first draft of the manuscript. JC, LZ, and YY performed the experiments, collected the data and drew figures. SH and XL interpreted the data. TL and SZ supervised the experiments. SZ, KHN and CR revised the manuscript. All authors read, revised and approved the final manuscript.

COMPETING INTERESTS

The authors declare no competing interests.

ADDITIONAL INFORMATION

Supplementary information The online version contains supplementary material available at https://doi.org/10.1038/s41396-023-01383-3.

Correspondence and requests for materials should be addressed to Shungui Zhou.